# Brugada Syndrome Disease Phenotype Explained in Apparently Benign Sodium Channel Mutations

**Running title:** *Hoshi et al.; Atypical Mutations in Brugada Syndrome*

Malcolm Hoshi, BA[1,2]; Xi X. Du, BS[1]; Krekwit Shinlapawittayatorn, MD, PhD[1,2,3];

Haiyan Liu, MD[1]; Sam Chai, BS[1,2]; Xiaoping Wan, MD, PhD[1]; Eckhard Ficker, PhD[1]†;

Isabelle Deschênes PhD[1,2]

[1]The Heart and Vascular Research Center, Department of Medicine, MetroHealth Campus, [2]Department of Physiology & Biophysics, Case Western Reserve University, Cleveland, OH; [3]Cardiac Electrophysiology Research & Training Center, Faculty of Medicine, Chiang Mai University, Thailand
†Deceased

**Correspondence:**

Isabelle Deschênes, PhD

Heart and Vascular Research Center MetroHealth Campus

Case Western Reserve University

2500 MetroHealth Drive

Rammelkamp 614

Cleveland, OH 44109-1998

Tel: (216) 778-5166

Fax: (216) 778-1261

E-mail: ideschenes@metrohealth.org

**Abstract:**

***Background -*** Brugada syndrome (BrS) is an arrhythmogenic disorder that has been linked to mutations in *SCN5A*, the gene encoding for the pore-forming α-subunit of the cardiac sodium channel. Typically, BrS mutations in *SCN5A* result in a reduction of sodium current with some mutations even exhibiting a dominant-negative effect on wild-type (WT) channels thus leading to an even more prominent decrease in current amplitudes. However, there is also a category of apparently benign ("atypical") BrS *SCN5A* mutations that *in vitro* demonstrates only minor biophysical defects. It is therefore not clear how these mutations produce a BrS phenotype. We hypothesized that similar to dominant-negative mutations atypical mutations could lead to a reduction in sodium currents when co-expressed with WT to mimic the heterozygous patient genotype.

***Methods and Results -*** WT and "atypical" BrS mutations were co-expressed in HEK293 cells, showing a reduction in sodium current densities similar to typical BrS mutations. Importantly, this reduction in sodium current was also seen when the atypical mutations were expressed in rat or human cardiomyocytes. This decrease in current density was the result of reduced surface expression of both mutant and WT channels.

***Conclusions -*** Taken together, we have shown how apparently benign *SCN5A* BrS mutations can lead to the ECG abnormalities seen in BrS patients through an induced defect that is only present when the mutations are co-expressed with WT channels. Our work has implications for risk management and stratification for some *SCN5A*-implicated BrS patients.

**Introduction**

Brugada syndrome (BrS) is a potentially fatal arrhythmogenic disorder characterized on the electrocardiogram by ST-segment elevation in the right precordial leads.[1] Although afflicted patients have structurally normal hearts, they are predisposed to sudden cardiac death (SCD). It has been estimated that the syndrome is responsible for at least 20% of SCD in patients with structurally normal hearts and at least 4% of all sudden deaths.[2, 3] BrS is typically inherited in an autosomal dominant fashion[3] and currently, mutations in at least twelve different genes have been implicated as causes of this disorder.[4] Irrespective of the genes involved, the BrS ECG phenotype is ultimately catalyzed by an imbalance of the inward and outward currents during phase 1 of the cardiac action potential.[2] Mutations in the *SCN5A* gene encoding the cardiac sodium channel $Na_v1.5$ are the predominant source of inherited BrS, accounting for about 20-30% of all BrS cases.[4]

In general, *in vitro* experiments in heterologous expression systems show that *SCN5A* BrS mutations result in a major loss of sodium current and are thus able to explain the BrS phenotype of afflicted patients. Nevertheless, apparently benign *SCN5A* BrS mutations exist that do not exhibit this typical loss-of-function phenotype but rather display only small biophysical defects, if any. Consequently, defects in these "atypical" mutations appear insufficient to support the BrS ECG phenotype and explain the clinical manifestation of BrS in mutation carriers. This observation led us to question the nature of these mutations and ask how atypical *SCN5A* BrS mutations may cause a BrS phenotype despite near normal channel behavior.

Some typical (loss-of-function) *SCN5A* BrS mutations have a dominant-negative effect on WT channels therefore leading to an even more prominent decrease in sodium currents.[5, 6] Importantly, we have shown that the mechanism by which an *SCN5A* BrS mutation can produce

a dominant-effect on the WT channel involves some level of interaction between two α-subunits.[6] Moreover, work from our group and others has shown that a sodium channel polymorphism can modulate biophysical and trafficking defects in a variety of *SCN5A* mutations located on separate alleles.[7-9] Finally, Tester *et al* [10] reported a *SCN5A* mutation that -despite having normal physiological characteristics when expressed alone- produced a pathogenic effect when expressed in the presence of a common sodium channel polymorphism. Based on this information, we hypothesized that atypical BrS mutations may produce significant reductions in sodium currents when co-expressed with WT, thus explaining the manifestation of the disorder.

To mimic the heterozygous genotype usually present in patients, we co-expressed atypical *SCN5A* BrS mutations with WT channels and explored whether their biophysical and functional properties were modified. In fact, we found numerous atypical *SCN5A* BrS mutations that, although mainly innocuous and indistinguishable from WT channels when expressed alone, demonstrated significant reductions in total sodium current density when co-expressed with WT channels. The current reductions observed on co-expression explain the BrS disease phenotype, as it is similar in magnitude to what is observed for typical loss-of-function mutations. Importantly, we have unveiled how apparently benign *SCN5A* BrS mutations with minimal biophysical defects led to an emergent loss-of-function as a result of interaction between mutant and WT channels. This mechanism reconciles the phenotype of atypical mutations with total sodium current amplitude, and can explain the clinical manifestation of Brugada Syndrome seen in afflicted patients.

## Methods

### Cloning of SCN5A mutations

The N70K, R225W, E439K, R526H, G552R, E555K, L567Q, R620C, T632M, A647D, P701L,

R965H, R1023H, E1053K, A1113V, S1140T, D1275N, G1319V, L1501V, G1502S, and E1938K mutations were created using the Stratagene QuickChange XL Site Directed Mutagenesis Kit in the *SCN5A* background (PubMed Accession No.NM 198056) expressed in the GFP-IRES vector (BD Biosciences Clonetech, San Jose, CA).

**Expression of SCN5A in heterologous expression systems**

Cardiac sodium channel were expressed using transient transfections of mutant *SCN5A* together with GFP either in human embryonic kidney cells (HEK293), Chinese Hamster Ovary (CHO) cells, neonatal rat ventricular myocytes (NRVM), or iCell cardiomyocytes (Cellular Dynamics International, Madison, WI). Co-expression of WT was achieved using a CFP-tagged WT channel. Transfection of HEK293 and CHO cells was performed using the Polyfect Transfection Kit (Qiagen, Valencia, CA) according to the manufacturer's protocol. The total DNA transfected was equal to 0.3μg for both single and co-transfections. (A 1:1 ratio was used for co-transfections.) Transfection of either iCells or NRVMs was accomplished using Lipofectamine 2000 (Life Technologies, Grand Island, NY) according to manufacturer's protocol, using 1.2 μg DNA/35 mm dishes.

**Cellular electrophysiological measurements for functional characterisation**

Sodium currents from transfected cells were recorded one day after transfection at room temperature (22°C to 23°C) in the whole-cell configuration of the patch-clamp technique. Patch electrodes were prepared from 8161 Corning glass (Dow-Corning, Midland, MI) and the resistances of the electrodes were 1.5-2.5MΩ. To minimize voltage-clamp errors, series resistance compensation of Axopatch 200A was performed to values >85%. To generate voltage-clamp command pulses, PCLAMP version 10 (Molecular Devices, Sunnyvale, Calif) was used. The intracellular solution contained (in mmol/L, at pH 7.4): NaCl 35, CsF 105, EGTA 10, and

Cs-HEPES 10. The external solution for HEK293 and CHO cells contained (mmol/L): NaCl 140, KCl 5, MgCl$_2$ 1, CaCl$_2$ 2, glucose 10, and HEPES 10 (pH 7.4). For NRVM and iCells, a low sodium external solution was used containing 35 mM sodium.

Whole-cell $I_{Na}$ densities and current-voltage relationships were recorded by holding the resting membrane potential at -120mV and stepping in 10mV intervals from -80 to +60mV for 30ms. Steady-state inactivation was elicited using 500ms prepulses in the range of -140mV to +60mV in 10mV increments followed by a 30ms test pulse to -30mV. Time course of recovery from inactivation ($\tau_{rec}$) was studied using a 2-pulse protocol with a 30ms prepulse to -30mV with varying rest intervals at -120mV, followed by a 30ms test pulse to -30mV.

Block by extracellular applications of [2-(trimethylammonium) ethyl] methanethiosulfonate bromide (MTSET) (2 μMol/L) was measured using a 30ms test pulse to -30mV. Percent of block was obtained by comparing residual currents after 10 minutes exposure to MTSET to currents before application of the drug.

**Data Analysis**

Data acquisition of voltage clamp data was performed using Clampex 10 (Molecular Devices, Union City, CA, USA). Off-line data analysis was performed with Clampfit 10 (Molecular Devices) and Origin 8.5.1 (OriginLab Corp., Northampton, MA, USA). For recovery from inactivation, peak current amplitude was fit to the following equation:

$$I_{test}/I_{pre\text{-}pulse} = 1 - \exp(-t/\tau_{rec})$$

For steady-state inactivation, normalized currents were fit to a Boltzmann distribution:

$$I/I_{max} = (1 + \exp[(V-V_{1/2})/k_v])^{-1}$$

For measurements of current density, after entering whole-cell mode, a 10mV pulse was administered to each cell to determine capacitance as area under the curve (pF). Experimentally determined capacitance was used to normalize currents evoked from each cell (pA/pF).

**Cell Surface Biotinylation**

3x100mm dishes of HEK293 cells were transfected with 2.5µg DNA for each separate construct/dish. Cells were collected 48h post-transfection, washed three times with PBS. Biotinylation was performed in 10 mL ice-cold PBS containing 0.25 mg/mL sulf-NHS-SS-Biotin for 30 minutes at 4°C. 10mM glycine was added to quench the reaction. Cell lysis solution contained (in mM/L) 50 HEPES (pH 7.4), 150 NaCl, 1.4 MgCl2, 1 EGTA, 10% Glycerol, 1% triton X-100, 1.2mg/mL N-Ethyl-maleimide with protease inhibitors. NeutrAvidin Agarose was used to pull down labeled proteins. Eluted proteins were then used for Western blotting as previously described,[11] and blotted using a sodium channel antibody (Millipore Polyclonal Anti-Na+ Channel III-IV loop). Pan-cadherin (Cell Signaling Technology) was used as a loading control for the cell surface biotinylated fraction and actin (Sigma-Aldrich monoclonal Anti-Actin, Clone AC-40) was used as a negative control for the cell surface biotinylated fraction. To determine the protein expression level, the sodium channel bands were normalized to the control bands (actin for total lysate and pan-cadherin for biotinylated fractions).

**Co-immunoprecipitation**

Co-IP experiments were carried out using Dynabeads from Invitrogen (Life Technologies) as previously described.[6] Briefly, washed magnetic beads were added to lysed HEK293 cells expressing the construct of interest. Immunoglobulin capture was carried out for 60' at room temperature (22-23°C) or overnight at 4°C using Protein G to control for non-specific binding. Target-bound beads were then incubated for 30 minutes at 37° and the supernatant used for

Western blot as previously described.[11] An HA antibody (Roche monoclonal Anti-HA high affinity antibody) was used for the immunoprecipitation and the blots were revealed with a GFP antibody (Clontech GFP monoclonal antibody).

**Neonatal Rat Myocytes**

Neonatal rat cardiac myocytes were isolated from 1- or 2-day old Sprague-Dawley rats and cultured as previously described.[12] Cells were transfected 48h after plating and used 24h post-transfection for patch-clamp experiments. The neonatal rat procedures followed were in accordance with institutional guidelines.

**iCells Cardiomyocytes**

Induced cardiomyocytes from Cellular Dynamics were cultured at 37°C in 7% $CO_2$ according to the manufacturer protocol. Transfections were carried out using Lipofectamine 2000 as described above. Patch clamp experiments were carried out 24-36h post-transfection.

**Statistical Analysis**

For sample sizes >10, statistical analysis was performed using the standard statistical package available in Origin 8.5.1 using parametric $t$-tests with a critical value <0.05 considered significant after determining normality with the Shapiro-Wilk test. For sample sizes <10, the Mann-Whitney U test was performed using Minitab 16 Statistical Software.

**Results**

**Functional analysis of atypical BrS mutations with and without wild-type channels**

Putative atypical mutations were selected from the Inherited Arrhythmias Database website (www.fsm.it/cardmoc). We first characterized the biophysical properties of these BrS mutations expressed alone and confirmed that they express currents largely indistinguishable from WT. We then expressed the so-called "atypical" BrS mutations with and without WT in HEK293 and

recorded whole-cell currents. Figure 1A shows representative Na$^+$ current traces ($I_{Na}$) recorded from WT, the atypical mutation L567Q, and L567Q+WT. In these experiments, current density was similar for WT and L567Q (Figure 1B). However, upon co-expression of L567Q with WT *SCN5A*, we observed a decrease in current density when compared to WT or L567Q alone (Figure 1A-B). Furthermore, our analysis showed no statistically significant difference in either steady-state inactivation or recovery from inactivation between WT, L567Q, and L567Q+WT (Table 1). Additional experiments were performed in CHO cells to exclude the possibility that our observations were restricted to channels expressed in HEK293 cells. Results were similar in CHO cells, with a reduction in current density on co-expression of L567Q with WT (Figure 1B).

**Functional analysis of the atypical mutation, L567Q, in neonatal rat ventricular myocytes (NRVM)**

To determine if the results observed in Figure 1 were also true for myocytes and not just an artifact of the expression system, NRVMs were transfected with either "atypical" L567Q or WT cDNA (Figure 2A). While transfection of WT Nav1.5 in NRVM produced the expected increase in sodium currents (Figure 2A-B), expression of L567Q in NRVMs produced a reduction in sodium currents, re-capitulating the current reduction seen in HEK293 cells (Figure 2A-B). Thus, we conclude that the current reduction seen with the atypical mutant on co-expression with WT is not an artifact of HEK293 cells but is preserved in an endogenous cardiac background.

**Functional analysis of atypical mutation L567Q in human cardiomyocytes**

Next we asked whether our results in NRVMs also hold true in human cardiomyocytes. In these experiments we utilized iCell cardiomyocytes (Cellular Dynamics International, Madison, WI). These cells are human induced pluripotent stem cell derived cardiomyocytes of high purity and preserve many properties of native human cardiac myocytes. Figure 2C shows I/V curves

obtained after transfecting either atypical mutant L567Q or GFP (control) in these human induced pluripotent stem cell derived cardiomyocytes. Current density was reduced when the atypical BrS mutation was expressed in these human cardiomyocytes compared to control transfections with GFP (Figure 2C). Again, our data are consistent with results obtained from NRVMs or HEK293 cells on heterologous expression of the respective mutant channels.

**Identification of Additional Atypical BrS Mutations**

To expand on our initial observations with L567Q we screened for additional atypical BrS mutations. We found that N70K, E439K, G552R, E555K, A647D, R965H, E1053K, S1140T, L1501V, G1502S, and E1938K produced a reduction in sodium current density upon co-expression with WT (Figure 3A). In general, on co-expression atypical mutations showed a reduction in peak current densities ranging from 30 to 70% when compared to mutations expressed alone (Figure 3A). As can be seen in Table 1, the biophysical properties of all mutations studied including recovery from inactivation ($\tau_{rec}$) and steady-state inactivation ($V_{1/2}$) parameters varied only minimally. Notably, in our screen we also identified atypical mutations with minimal defects whose current amplitude did not change upon co-expression with WT in HEK293 cells (Figure 3B). To confirm these results obtained in HEK293 cells, we expressed in human cardiomyocytes two atypical mutations: E555K (which led to a reduction in total currents when co-expressed with WT) and T632M (which did not reduce currents when co-expressed with WT). We found, as expected, that total sodium current density was reduced in human cardiomyocytes when E555K was transfected in these cells (Figure 3B). In marked contrast, when T632M was transfected in human cardiomyocytes, total sodium current densities were not significantly different from control transfections with GFP, hence confirming the results obtained in HEK293 cells (Figure 3C).

**Cell Surface Biotinylation and Co-Immunoprecipitation**

The current reductions observed on co-expression of WT sodium channel with atypical BrS

mutants may be attributed either to (1) a decrease in protein synthesis or (2) an induced

trafficking defect of WT and/or atypical mutant channels. To discriminate between WT and

atypical mutant channels, we used a WT channel fused to YFP, which increases the size of the

channel protein. To assess changes in protein synthesis, WT-YFP and the atypical mutants

L567Q and E555K were expressed either alone or on co-transfection. Figure 4A shows that total

protein levels were maintained which indicates that current reductions were not due to a decrease

in protein synthesis. In a second step, cell surface biotinylation was performed to determine

whether the level of channel proteins present at the cell surface membrane was modified. We

found that WT, E555K and L567Q showed similar protein levels at the cell surface, as expected

based on similar current densities (Figure 4A). However, co-expression of WT with either

atypical mutation drastically reduced cell surface expression of both WT and mutant channels

(Figure 4A), suggesting that the reduction in currents is due to induced trafficking defects of both

WT and mutant channels. As a negative control to demonstrate the purity for cell-surface protein

of our biotinylated fraction, the blots were also probed for the cytosolic protein actin. The

absence of an actin signal in the surface fractions and the presence of an actin signal in the total

cell lysate fractions confirmed the accuracy of the fractions. Additionally, pan-cadherin was

used as a loading control for the cell surface biotinylated fraction. We have previously shown

that sodium channels associate with each other which may explain the dominant-negative effect

exerted by a BrS mutant on WT.[6] Similarly, we used co-immunoprecipitation to test whether

channel interactions were conserved between WT and atypical BrS mutants and found that this

interaction was indeed maintained between WT and the atypical L567Q mutant (Figure 4B).

**Electrophysiological hallmarks co-expressing L567Q and WT**

Our surface biotinylation experiments demonstrated a drastic reduction in surface membrane

protein of both WT and mutant channels which in itself would explain the reduction in current

amplitudes observed. However, surface biotinylation experiments do not guarantee that both

channels are functional at the level of the cell surface membrane. Therefore, we tested the

functionality of both mutant and wild-type sodium channels using a WT-C373Y construct

resistant to block by MTSET. MTSET ordinarily inhibits sodium channels by binding to a

cysteine at residue 373.[13-15] Mutating residue C373 to tyrosine (C373Y) has been shown to

essentially eliminate sensitivity to extracellular applications of MTSET.[8] Thus, upon co-

expression with L567Q, selective mutation of WT-C373Y will render only WT current

insensitive to MTSET.

Figure 5 shows representative sodium current recordings of WT-C373Y and L567Q in the

absence and presence of 2 μmol/L of MTSET. After addition of MTSET, drug effects were

allowed to reach steady-state prior to current measurements. As expected, WT-C373Y alone did

not show any significant decrease in peak current density, while L567Q was blocked to a large

extent (Figure 5 A-B). More importantly, on co-expression MTSET reduced sodium current

density by about 50% at steady state (Figure 5 A-B). As this decrease in peak current density can

be attributed only to block of L567Q, our results suggest that both channels are functional at the

cellular surface and present at similar levels.


**Discussion**

Mutations in the *SCN5A* gene encoding the cardiac sodium channel $Na_v1.5$ are implicated in

multiple cardiac diseases, including fatal arrhythmogenic disorders such as Long QT syndrome

Type 3 and Brugada Syndrome. The BrS ECG phenotype is most often the result of loss-of-

function in Na$_v$1.5. BrS typically manifests *in vitro* as a loss of whole-cell sodium currents, and

*in vivo* as conduction slowing. In marked contrast, we describe here a category of putative

*SCN5A* BrS mutations which are apparently benign (hence "atypical" mutations). These atypical

mutations do not reduce current density *in vitro* as typical *SCN5A* BrS mutations do and when

they do, it is to such a small extent that they appear insufficient to produce a BrS phenotype. In

addition, their biophysical properties of voltage-current relationship, steady-state inactivation,

and recovery from inactivation remain relatively unchanged. However, we have now

demonstrated that co-expression of many atypical mutations with wild-type *SCN5A* result in a

counterintuitive *decrease* of current density. This decrease in current density is not the result of

defective biosynthesis. Instead, our surface biotinylation experiments show a reduction in cell

surface expression of both WT and mutant proteins on co-expression of atypical mutations with

WT channels. This is also reflected in our MTSET experiments showing that while current

density is reduced on co-expression, both WT and mutant channels are not only present but also

functional. Taken together, our analysis suggests that the loss of current density upon co-

expression with WT is the result of an induced trafficking defect affecting both mutant and WT

channels.

It is apparent that the mechanism governing the behavior of atypical BrS mutations relies

on a damaging interaction between two otherwise normally functioning α-subunits. This

observation is surprising, because it deviates from the established paradigms of

haploinsufficiency or negative dominance. To the best of our knowledge, no such mechanism has

been previously reported. On a more mechanistic level we speculate that there is either (i) a

misfolding event that occurs when a WT channel interacts with a mutant channel thereby

impairing forward trafficking, (ii) a symmetry-sensing event which allows only for successful

processing and export of like-channel pairs or (iii) increased degradation of both channels when co-expressed. However, those potential mechanisms are all hypothetical and need to be further explored.

Interestingly, the atypical mutations that displayed a loss of current density upon co-expression with WT were located exclusively on the cytoplasmic domains of the channel (Figure 6, circles). This observation becomes more intriguing as one has to consider that $Na_V1.5$ is known to interact with a host of binding partners via its cytoplasmic domains,[16, 17] suggesting that the α-subunits may have interaction mediated by one or more of these binding partners. This represents other potential pathways through which two independently perfectly functional channels may become non-functional on co-expression. Theoretically, disabling the interaction between atypical BrS and WT sodium channels may restore trafficking and ameliorate the disease phenotype clinically, as channel function is normal in isolation. Further work will seek to examine the role of these interacting proteins on producing the BrS loss-of-function phenotype from atypical BrS mutations.

Our findings appear to contrast a recent report by Mercier *et al* who found that for a dominant negative mutation located on the extracellular loop of DIII, the β1-subunit appeared to be required for α-α interaction.[18] However, our biochemical and patch clamp experiments here show interaction between α-subunits without co-transfection of β1-subunits and we have also previously demonstrated that co-immunoprecipitation between sodium channels was possible without β1-subunit over expression.[6] Despite extensive debate within the sodium channel community, the physiological effects of the β1-subunit remain poorly understood. Further complicating matters is the fact that HEK293 cells are known to endogenously express β1-subunits in a highly variable manner. Therefore, one potential explanation for the discrepancy

between our work and that of Mercier *et al* could be due to different endogenous levels of β1-subunits present in the expression systems used.

A loss-of-function in *SCN5A* arising directly from the interaction of a disease allele with WT is attractive as it offers an elegant solution for apparently innocuous BrS mutations showing WT-like behavior. However, not all mutations without loss of function characteristics showed a current reduction upon co-expression with WT. One possible explanation is the uncertainty of these mutations being benign polymorphisms instead of 'true' BrS mutations. Importantly, even though these *SCN5A* variants have been putatively found in BrS patients, several of them have only been reported as 'candidate' gene mutations in the Inherited Arrhythmias Database (www.fsm.it/cardmoc). Thus, there is a distinct possibility that these mutations are not truly the source of the disease, especially when we consider the fact that no obvious functional defects have been reported on co-expression with WT in a heterologous system or in human cardiomyocytes.

Most importantly, however, our study demonstrates that *SCN5A* mutations may not only affect their own expression but also reduce expression of WT/mutant channels complexes in a heterozygous situation. Overall, our results have a high level of clinical significance in that they offer a novel mechanism to understand the complex phenomenon of genotype-phenotype discordance that was presented by these atypical mutations because it was up until now unclear how an *SCN5A* mutant channel with no major biophysical defects could lead to BrS. This genotype-phenotype discordance is of high interest to clinicians as it affects risk stratification and ultimately treatment options for BrS patient and closely related family members that are mutation carriers. While some progress has been made toward explaining the genotype-phenotype discordance of BrS (namely, the contribution of disease-modifying genes)[19] it remains

poorly understood. To this end, our present study identifies for the first time a pathophysiological mechanism for a number of atypical BrS *SCN5A* mutations and offers guidance for future treatment approaches similar to typical loss-of-function *SCN5A* BrS mutations.

**Conflict of Interest Disclosures:** None

**References:**

1. Brugada P, Brugada J. Right bundle branch block, persistent st segment elevation and sudden cardiac death: A distinct clinical and electrocardiographic syndrome. A multicenter report. *J Am Coll Cardiol*. 1992;20:1391-1396.

2. Benito B, Brugada J, Brugada R, Brugada P. Brugada syndrome. *Rev Esp Cardiol*. 2009;62:1297-1315.

3. Antzelevitch C, Brugada P, Borggrefe M, Brugada J, Brugada R, Corrado D, et al. Brugada syndrome: Report of the second consensus conference: Endorsed by the heart rhythm society and the european heart rhythm association. *Circulation*. 2005;111:659-670.

4. Nademanee K, Veerakul G. Brugada syndrome: Two decades of progress. *Circ J*. 2012;76:2713-2722.

5. Keller DI, Rougier JS, Kucera JP, Benammar N, Fressart V, Guicheney P, et al. Brugada syndrome and fever: Genetic and molecular characterization of patients carrying scn5a mutations. *Cardiovasc Res*. 2005;67:510-519.

6. Clatot J, Ziyadeh-Isleem A, Maugenre S, Denjoy I, Liu H, Dilanian G, et al. Dominant-negative effect of scn5a n-terminal mutations through the interaction of nav1.5 a-subunits. *Cardiovasc Res*. 2012;96:53-63.

7. Marangoni S, Rocchetti M, Barile L, Rizzetto R, Summa A, Severi S, et al. A Brugada syndrome mutation (p.S216l) and its modulation by p.H558r polymorphism: Standard and dynamic characterization. *Cardiovasc Res*. 2011;91:606-616.

8. Poelzing S, Forleo C, Samodell M, Dudash L, Sorrentino S, Anaclerio M, et al. Scn5a polymorphism restores trafficking of a brugada syndrome mutation on a separate gene. *Circulation*. 2006;114:368-376.

9. Shinlapawittayatorn K, Du XX, Liu H, Ficker E, Kaufman ES, Deschenes I. A common scn5a polymorphism modulates the biophysical defects of scn5a mutations. *Heart Rhythm*. 2011;8:455-462.

10. Tester DJ, Valdivia C, Harris-Kerr C, Alders M, Salisbury BA, Wilde A, et al. Epidemiologic, molecular, and functional evidence suggest a572d-scn5a should not be considered an independent lqt3-susceptibility mutation. *Heart Rhythm*. 2010;7:912-919.

11. Shinlapawittayatorn K, Dudash LA, Du XX, Heller L, Poelzing S, Ficker E, et al. A novel strategy using cardiac sodium channel polymorphic fragments to rescue trafficking-deficient scn5a mutations. *Circ Cardiovasc Genet.* 2010;4:500-509.

12. Deschenes I, Armoundas AA, Jones SP, Tomaselli GF. Post-transcriptional gene silencing of kchip2 and navbeta1 in neonatal rat cardiac myocytes reveals a functional association between na and ito currents. *J Mol Cell Cardiol*. 2008;45:336-346.

13. Chen LQ, Santarelli V, Horn R, Kallen RG. A unique role for the s4 segment of domain 4 in the inactivation of sodium channels. J Gen Physiol. 1996;108:549-556.

14. Satin J, Kyle JW, Chen M, Bell P, Cribbs LL, Fozzard HA, et al. A mutant of ttx-resistant cardiac sodium channels with ttx-sensitive properties. *Science*. 1992;256:1202-1205.

15. Sheets MF, Hanck DA. Molecular action of lidocaine on the voltage sensors of sodium channels. *J Gen Physiol*. 2003;121:163-175.

16. Abriel H. Cardiac sodium channel nav1.5 and interacting proteins: Physiology and pathophysiology. *J Mol Cell Cardiol.* 2010;48:2-11.

17. Abriel H, Kass RS. Regulation of the voltage-gated cardiac sodium channel nav1.5 by interacting proteins. *Trends Cardiovasc Med.* 2005;15:35-40.

18. Mercier A, Clément R, Harnois T, Bourmeyster N, Faivre J-F, Findlay I, et al. The β1-Subunit of Nav1.5 Cardiac Sodium Channel Is Required for a Dominant Negative Effect through α-α Interaction. *PLoS ONE*. 2012;7:11e48690.

19. George AL. Molecular and genetic basis of sudden cardiac death. *J Clin Invest*. 2013;123:75-83.

**Table 1:** Biophysical properties of mutations studied. Table showing $V_{1/2}$ and $\tau_{rec}$ of mutations studied. P values represent a comparison between mutation alone and mutation + WT

| Mutation | $V_{1/2}$ (mV) | SEM | P | $\tau_{rec}$ (ms) | SEM | P | n |
|---|---|---|---|---|---|---|---|
| N70K | -79.62 | 0.64 | ns | 2.81 | 0.08 | ns | 19 |
| N70K+WT | -79.47 | 0.50 | | 2.89 | 0.15 | | 15 |
| R225W | -81.29 | 1.24 | ns | 3.49 | 0.23 | ns | 11 |
| R225W+WT | -79.80 | 1.36 | | 2.94 | 0.22 | | 10 |
| E439K | -80.00 | 0.53 | ns | 3.66 | 0.32 | ns | 11 |
| E439K+WT | -81.25 | 0.97 | | 3.61 | 0.16 | | 17 |
| R526H | -81.29 | 0.85 | ns | 3.88 | 0.14 | ns | 11 |
| R526H+WT | -80.60 | 1.78 | | 4.02 | 0.12 | | 10 |
| G552R | -81.23 | 0.97 | ns | 3.25 | 0.23 | ns | 15 |
| G552R+WT | -82.16 | 0.93 | | 3.25 | 0.23 | | 13 |
| E555K | -82.16 | 0.93 | ns | 3.28 | 0.09 | ns | 17 |
| E555K+WT | -82.26 | 0.92 | | 3.31 | 0.13 | | 15 |
| L567Q | -79.91 | 0.68 | ns | 3.49 | 0.14 | ns | 13 |
| L567Q+WT | -82.00 | 0.94 | | 3.86 | 0.16 | | 11 |
| R620C | -81.65 | 1.17 | ns | 4.11 | 0.10 | <0.05 | 11 |
| R620C+WT | -83.43 | 1.12 | | 3.75 | 0.07 | | 11 |
| T632M | -81.81 | 0.36 | <0.05 | 3.27 | 0.19 | ns | 10 |
| T632M+WT | -78.43 | 1.17 | | 3.30 | 0.20 | | 11 |
| A647D | -80.54 | 0.94 | ns | 2.90 | 0.20 | <0.05 | 10 |
| A647D+WT | -79.76 | 1.18 | | 3.34 | 0.10 | | 16 |
| P701L | -82.52 | 0.70 | ns | 3.93 | 0.20 | ns | 11 |
| P701L+WT | -83.66 | 1.06 | | 3.95 | 0.25 | | 10 |
| R965H | -79.78 | 0.62 | ns | 3.43 | 0.18 | ns | 12 |
| R965H+WT | -81.76 | 0.46 | | 3.25 | 0.13 | | 10 |
| R1023H | -77.23 | 0.56 | ns | 3.66 | 0.17 | <0.05 | 10 |
| R1023H+WT | -77.69 | 0.86 | | 2.81 | 0.14 | | 10 |
| E1053K | -75.77 | 1.24 | ns | 3.75 | 0.41 | ns | 11 |
| E1053K+WT | -76.60 | 1.15 | | 3.38 | 0.21 | | 13 |
| A1113V | -80.26 | 0.53 | ns | 3.45 | 0.19 | ns | 15 |
| A1113V+WT | -80.86 | 0.82 | | 3.08 | 0.16 | | 12 |
| S1140T | -82.53 | 1.09 | ns | 3.81 | 0.32 | <0.05 | 14 |
| S1140T+WT | -82.00 | 1.18 | | 2.96 | 0.16 | | 11 |
| D1275N | -80.32 | 1.29 | ns | 2.25 | 0.47 | <0.05 | 12 |
| D1275N+WT | -79.68 | 1.30 | | 4.12 | 0.19 | | 11 |
| G1319V | -81.40 | 0.53 | ns | 4.77 | 0.33 | <0.05 | 14 |
| G1319V+WT | -82.23 | 0.79 | | 3.82 | 0.21 | | 11 |
| L1501V | --79.29 | 1.41 | ns | 3.13 | 0.39 | ns | 13 |
| L1501V+WT | -78.35 | 0.80 | | 3.16 | 0.22 | | 15 |
| G1502S | -86.66 | 0.74 | ns | 4.95 | 0.21 | <0.05 | 14 |
| G1502S+WT | -84.30 | 0.62 | | 3.93 | 0.30 | | 10 |
| E1938K | -80.44 | 0.91 | ns | 3.09 | 0.18 | ns | 15 |
| E1938K+WT | -78.80 | 0.47 | | 2.94 | 0.22 | | 13 |
| WT | -79.48 | 0.60 | n/a | 3.58 | 0.20 | n/a | 18 |

**Figure Legends:**

**Figure 1:** Effect of WT on L567Q atypical mutation. A. Representative traces for SCN5A-WT, SCN5A-L567Q and SCN5A-L567Q+WT expressed in HEK293 cells. B. Summary of peak current density in HEK293 and CHO cells showing a reduction in peak current density upon co-expression with WT. Data presented as mean±SEM. (n= WT: 18, L567Q: 12, L567Q+WT: 14) Cells were transfected with 0.3μg total DNA; 0.3μg for mono-transfections or 0.15/0.15μg for co-transfections. (*$p<0.05$ compared to L567Q alone)

**Figure 2:** Expression of atypical BrS mutant sodium channels in myocytes significantly reduces sodium current density. A. Family of sodium current traces in NRVMs in response to a series of 30-ms test pulses. Control represents non-transfected cells. B. Summary of peak current density recorded at -20 mV. When SCN5A-L567Q was transfected in NRVM, the peak current was reduced by about 50% compared to non-transfected cells. (*$p<0.01$ compared to non-transfected cells) (n= control: 12, L567Q: 11, WT: 16). . C. iCells from Cellular Dynamics show a reduction of current upon transfection with L567Q, consistent with data from HEK293 cells. GFP transfected cells were used as a control. (n= GFP: 11, L567Q: 7, T632M: 8)

**Figure 3:** Additional Atypical BrS Mutations Studied. A. Summary showing peak current densities of additional atypical BrS mutations that demonstrated a reduction upon co-expression with WT. (n= N70K: 19, N70K+WT: 15, E439K: 11, E439K+WT: 19, G552R: 15, G552R+WT: 13, E555K: 17, E555K+WT: 15, A647D: 11, A647D+WT: 16, R965H: 12, R965H+WT: 11, E1053K: 11, E1053K+WT: 15, S1140T: 16, S1140T+WT: 11, L1501V: 13, L1501V+WT: 15,

G1502S: 10, G1502S+WT: 10, E1938K: 15, E1938K+WT: 13). B. Summary showing peak

current densities of atypical BrS mutations that did not reduce upon co-expression with WT.

(*$p < 0.05$ compared to mutation alone; #$p < 0.05$ compared to WT) (n=R223W: 11, R223W+WT:

10, R526H: 11, R526H+WT: 10, R620C: 11, R620C+WT: 11, T632M: 10, T632M+WT: 11,

P701L: 12, P701L+WT: 10, R1023H: 10, R1023H+WT: 11, A1113V: 15, A1113V+WT: 12,

D1275N: 12, D1275N+WT: 11, G1319V: 14, G1319V+WT: 11. C. iCells from Cellular

Dynamics show results consistent with results from HEK293 cells for E555K (A) and T632M

(B). GFP transfected cells were used as a control. (n= GFP: 11, E555K: 9, T632M: 8)
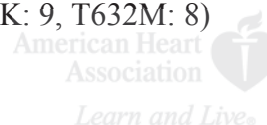
**Figure 4:** A. Surface Biotinylation Experiments. Whole-cell lysate (left) and surface

biotinylation fraction (right) for SCN5A-WT-YFP (2.5 μg), SCN5A-L567Q (2.5 g), SCN5A-

WT-YFP (2.5 g) + SCN5A-L567Q (2.5 g), SCN5A-E555K (2.5 g), and SCN5A-WT-YFP (2.5

g) + SCN5A-E555K (2.5 g). The Western was blotted with a sodium channel antibody. The

SCN5A-WT-YFP construct's size was around 260kDa whereas the mutations constructs were

around 220kDa. The cell surface biotinylation showed a dramatic reduction of both WT and

atypical mutations on co-expression, whereas the total protein level was not modified. Actin was

used as a negative control for the cell surface fractions and pan-cadherin was used as loading

control for the cell surface fractions. B Co-immunoprecipitation experiments were performed

between WT-YFP and a WT channel expressing an HA tag (WT-HA) and L567Q-YFP and WT-

HA. The pull down was performed with an HA antibody and the blot was revealed with a GFP

antibody. For both A and B, the figures are a representative example of at least three separate
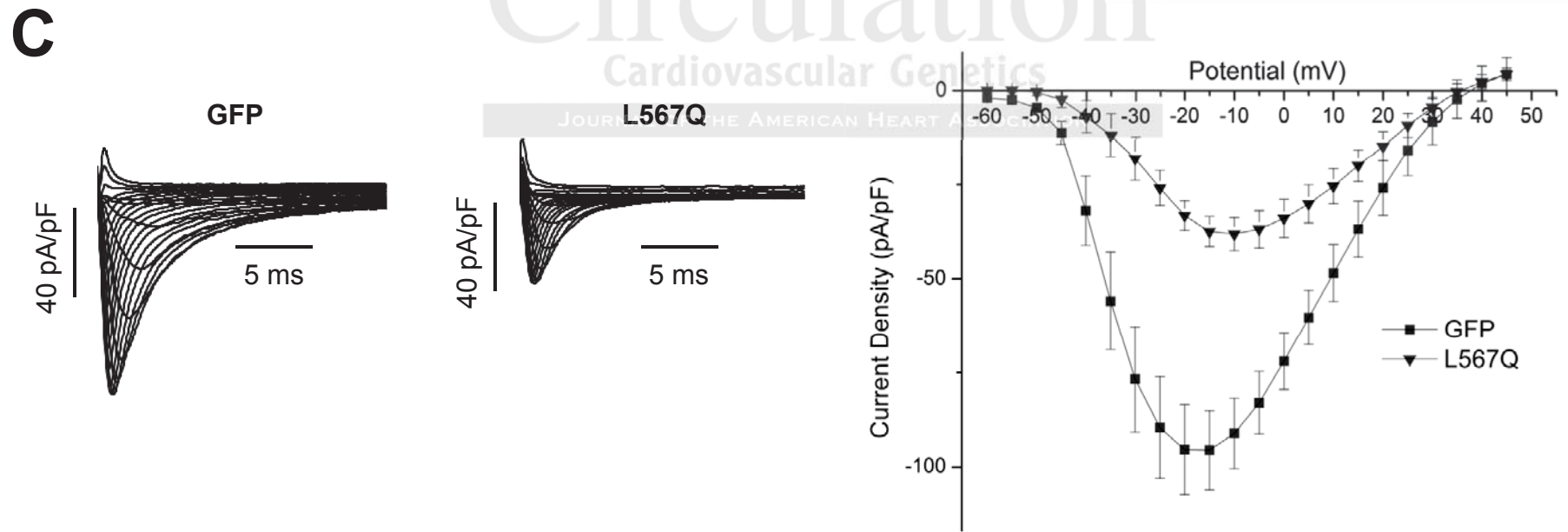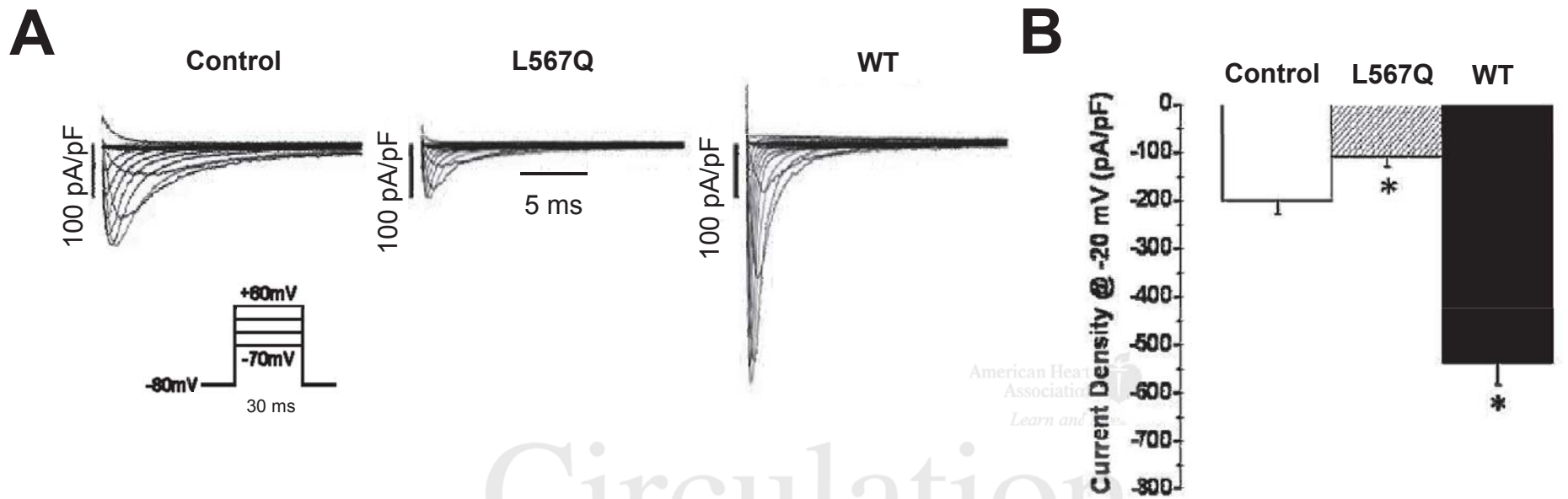
experiments.

**Figure 5:** Both WT and mutant channels are functional at the plasma membrane. A. Sodium currents before and after the addition of 2 μmol/L MTSET for SCN5A-C373Y (no reduction), SCN5A-L567Q (near total reduction) and SCN5A-L567Q+SCN5A-C373Y(~50% reduction) B. Averaged percent current reduction. There was no reduction in SCN5A-C373Y (n=10), a near complete reduction in SCN5A-L567Q (n=15), and a 58% reduction in SCN5A-L567Q+SCN5A-C373Y (n=15). These results demonstrate that both channels are present at the cell surface in a similar ratio. (*$p<0.05$ compared to SCN5A-C373Y).
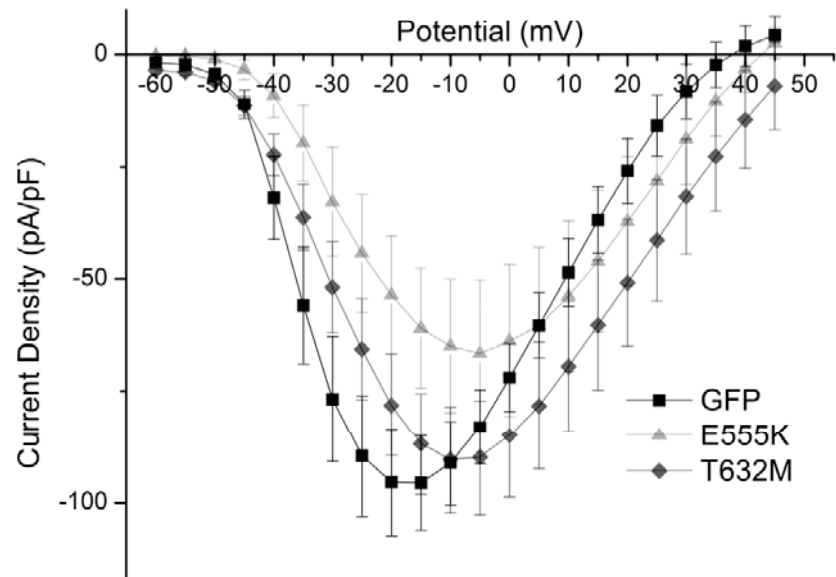
**Figure 6:** Schematic of Nav1.5 showing location of mutations studied. Atypical BrS mutations that showed no decrease in current density upon co-expression with WT are represented by squares, whereas atypical mutations showing a decrease in sodium currents when co-expressed with WT are represented by circles.

**A**

WT　　　　L567Q　　　　WT + L567Q

400 pA/pF　　　400 pA/pF　　　5 ms　　　400 pA/pF

+60mV
-80mV
-120mV
30 ms

**B**

HEK293 cells　　　　CHO cells

Peak Current Density (pA/pF)

WT
L567Q
L567Q+WT

*

**A**

C373Y    L567Q    L567Q + C373Y

500 pA    500 pA    500 pA

-30mV

-120mV

30 ms

5 ms

·········· + MTSET

**B**

% Current Reduction with MTSET

C373Y    L567Q    L567Q+C373Y

R225W

D1275N

S1140T

G1319V

P701L

E439K

A1113V

L1501V
G1502S

III-IV linker

R526H

R965H

G552R

E555K

R1023H

N70K

L567Q

A647D
T632M
R620C

E1053K

II-III linker

E1938K

NH₂

I-II linker

COOH
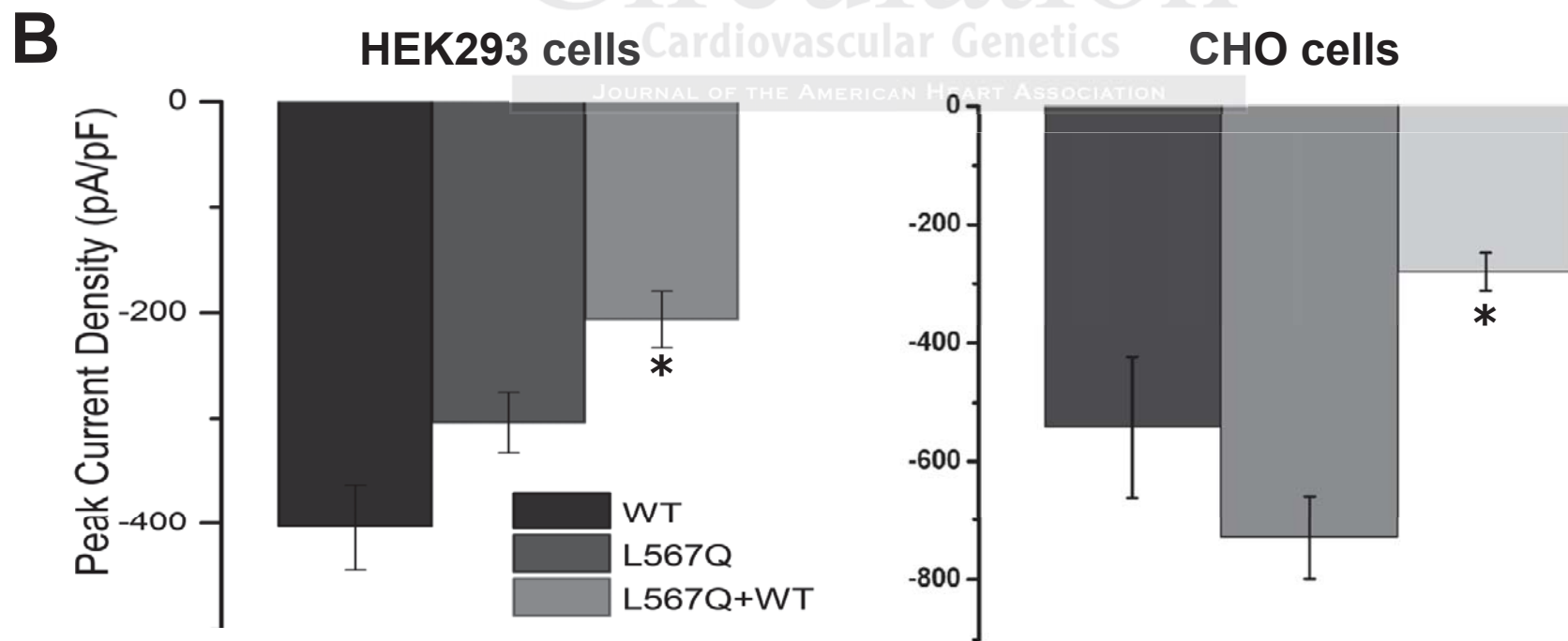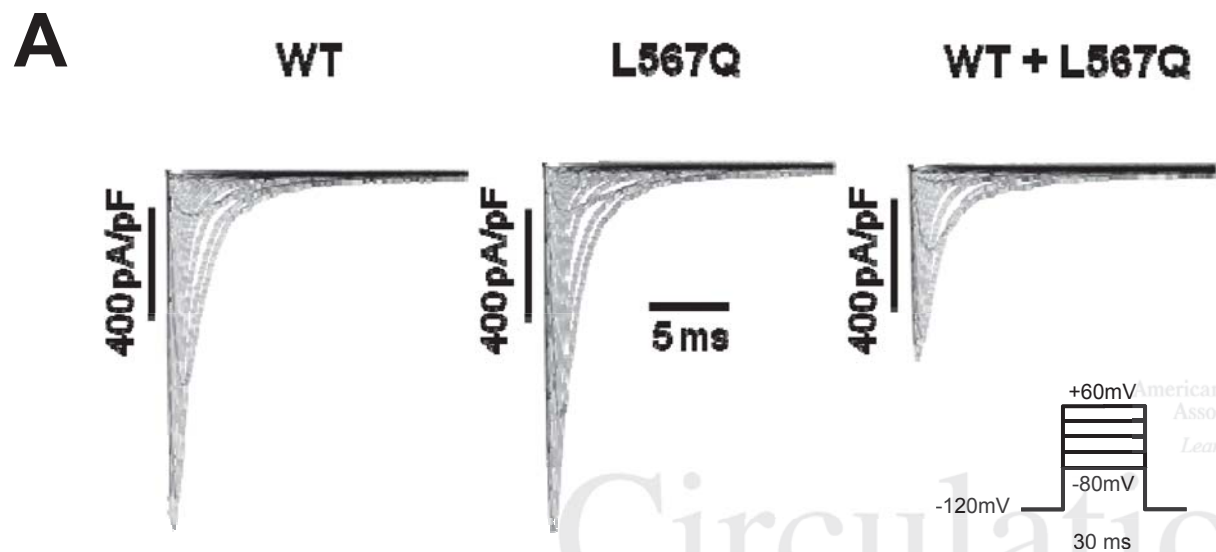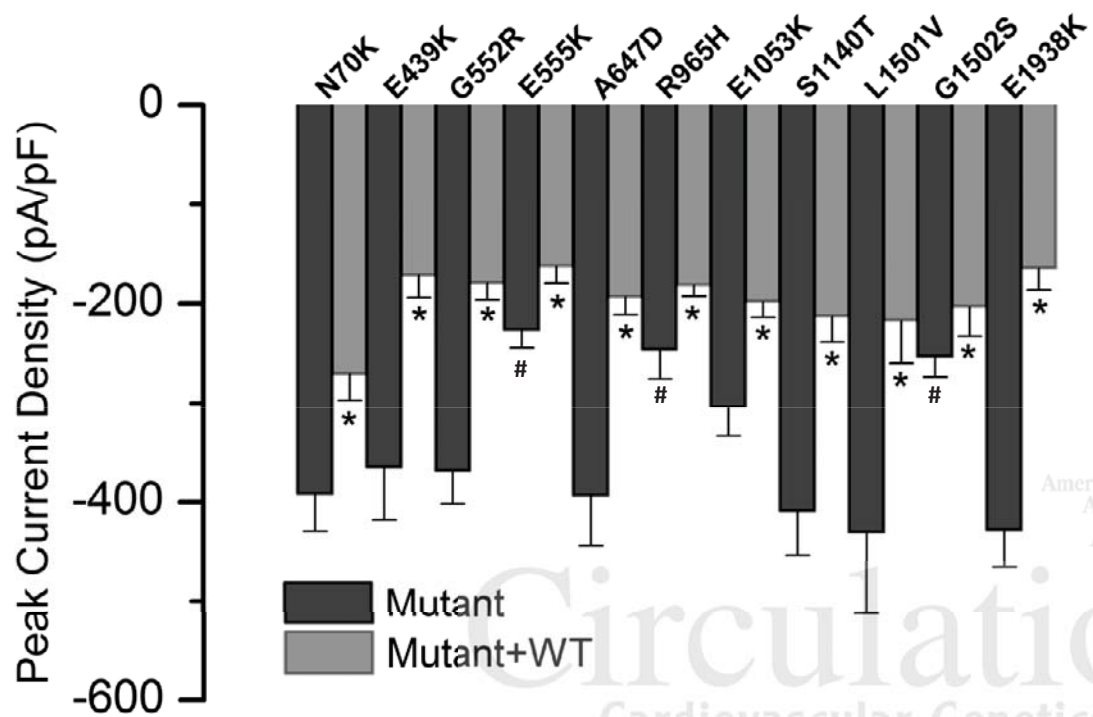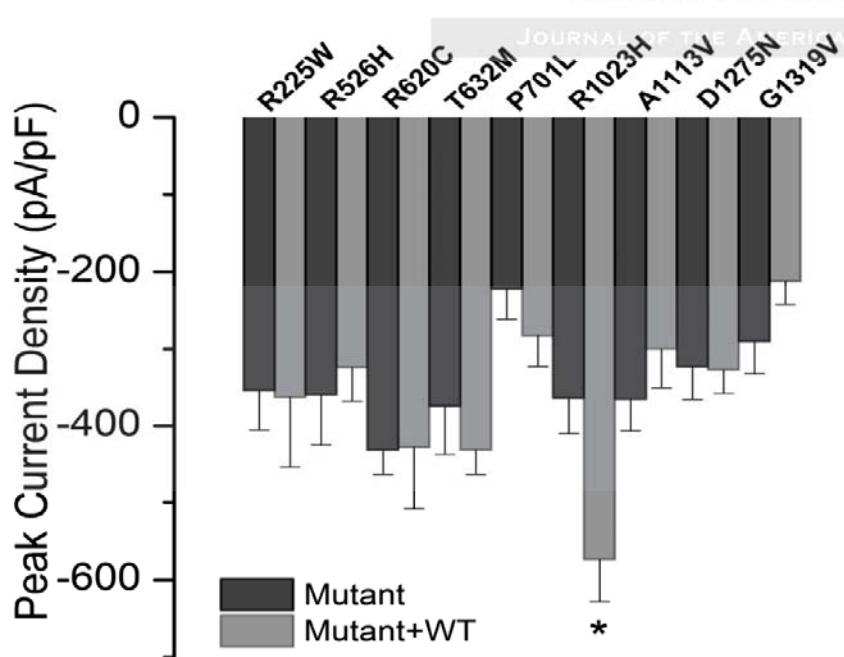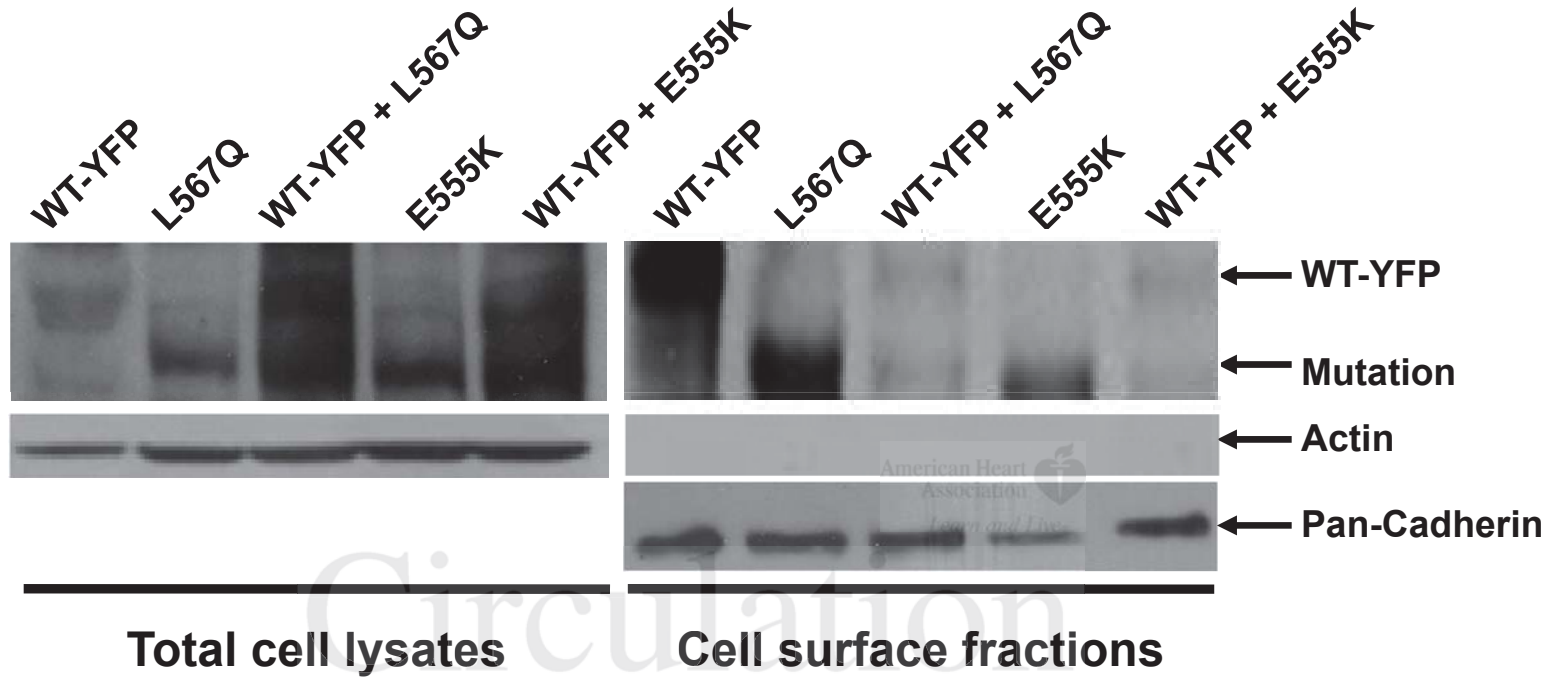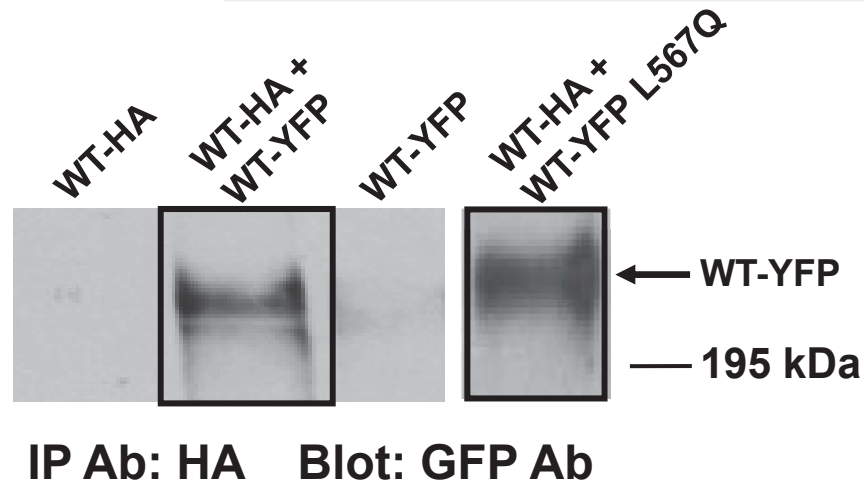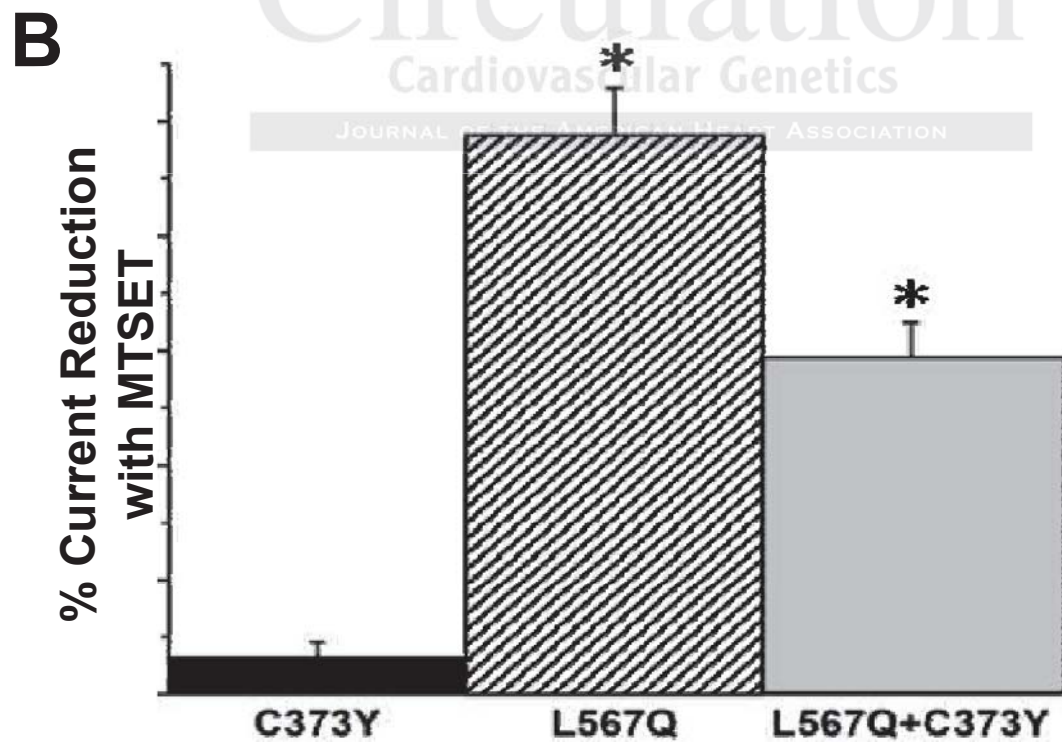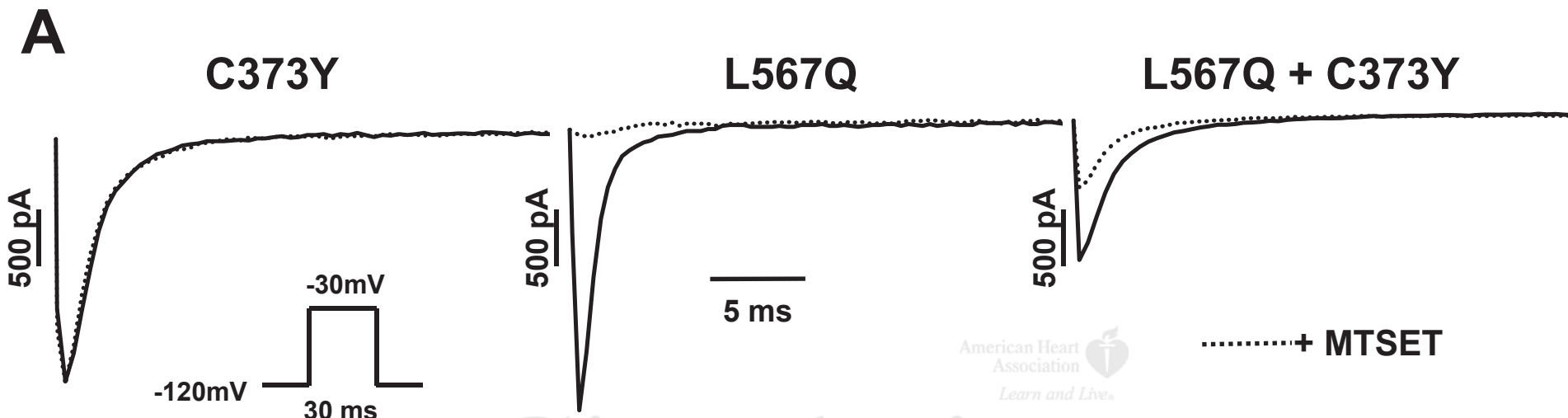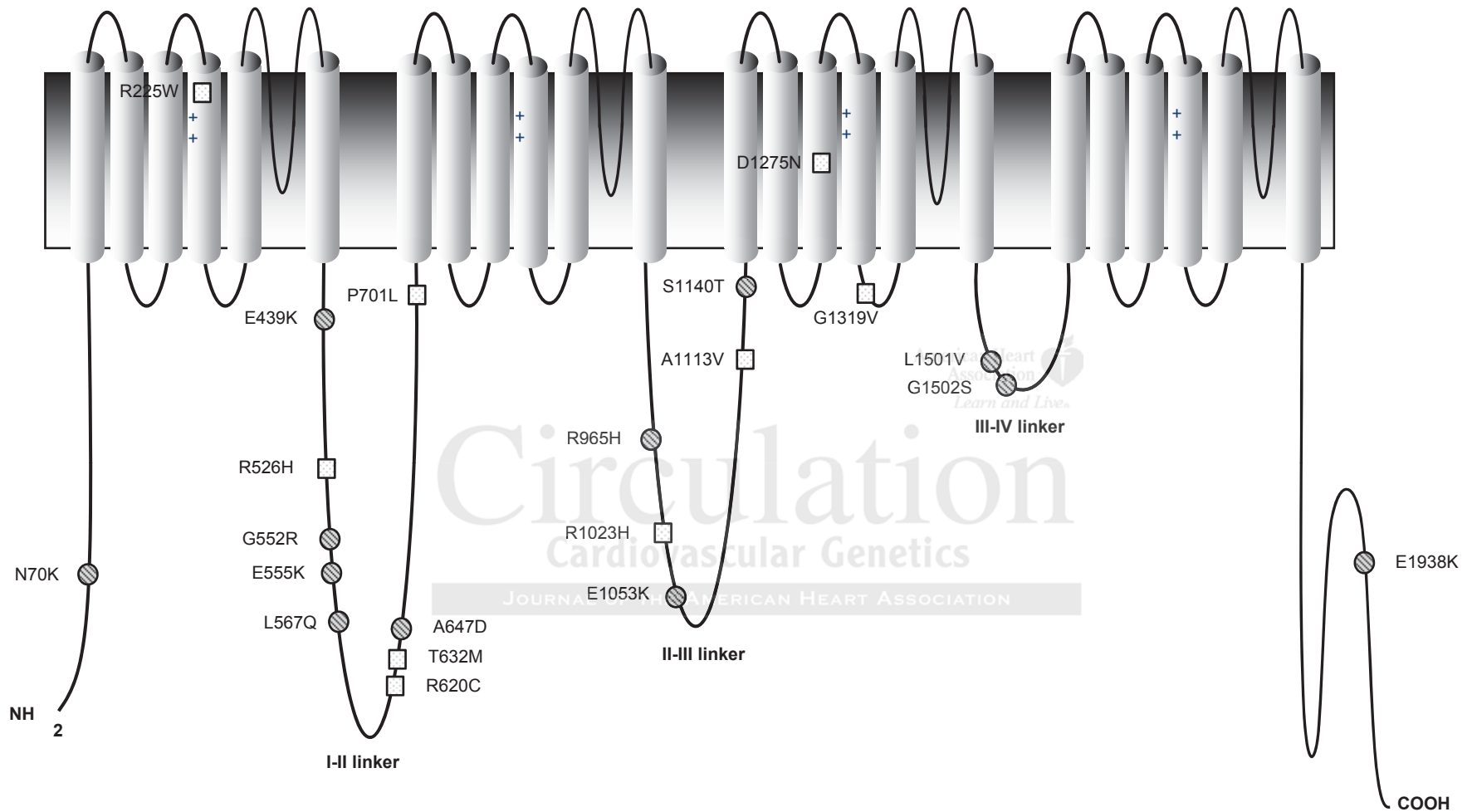
**Group I**  ☐ : Normal or larger peak $I_{Na}$ compared to WT when expressed alone or co-expressed with WT

**Group II** ◉ : Normal peak $I_{Na}$ when expressed alone, reduction of $I_{Na}$ upon co-expression with WT